Nanoscale Res Lett (2010) 5:930–934
DOI 10.1007/s11671-010-9584-3

NANO EXPRESS

# ZnSe/ZnSeTe Superlattice Nanotips

**C. H. Hsiao · S. C. Hung · S. H. Chih · S. B. Wang · Y. C. Cheng · B. R. Huang · S. J. Young · S. J. Chang**

Received: 17 February 2010 / Accepted: 16 March 2010 / Published online: 28 March 2010


**Abstract** The authors report the growth of ZnSe/ZnSeTe superlattice nanotips on oxidized Si(100) substrate. It was found the nanotips exhibit mixture of cubic zinc-blende and hexagonal wurtzite structures. It was also found that photoluminescence intensities observed from the ZnSe/ZnSeTe superlattice nanotips were much larger than that observed from the homogeneous ZnSeTe nanotips. Furthermore, it was found that activation energies for the ZnSe/ZnSeTe superlattice nanotips with well widths of 16, 20, and 24 nm were 76, 46, and 19 meV, respectively.

**Keywords** ZnSe/ZnSeTe superlattice nanotip · Photoluminescence · Activation energies

C. H. Hsiao · S. H. Chih · S. B. Wang · S. J. Chang (✉)
Institute of Microelectronics & Department of Electrical Engineering, Advanced Optoelectronic Technology Center, Center for Micro/Nano Science and Technology, National Cheng Kung University, Tainan 701, Taiwan
e-mail: changsj@mail.ncku.edu.tw

S. C. Hung
Department of Information Technology & Communication, Shih Chien University, Neimen, Kaohsiung 845, Taiwan

Y. C. Cheng
Materials and Electro-Optics Research Division, Chung Shan Institute of Science and Technology, Taoyuan 325, Taiwan

B. R. Huang
Graduate Institute of Electro-Optical Engineering, Department of Electronic Engineering, National Taiwan University of Science and Technology, Taipei 106, Taiwan

S. J. Young
Department of Electronic Engineering, National Formosa University, Huwei, Yunlin 632, Taiwan

## Introduction

Wide bandgap ZnSe-based II–VI materials are attractive materials that can be used in various optoelectronic applications. Using two-dimensional (2D) epitaxial layers, ZnSe-based light emitting diodes, laser diodes, and photodetectors have also been demonstrated [1–3]. Other than 2D epitaxial films, it is also possible to prepare one-dimensional (1D) ZnSe nanowires. With a large surface-to-volume ratio, 1D systems including nanowires and nanorods have attracted great interest in recent years. It is generally recognized that 1D materials are the ideal building blocks for novel nano-scaled optoelectronic devices. 1D ZnSe nanowires can be prepared by pulse laser deposition [4], metalorganic chemical vapor deposition [5], phase vapor growth [6], and molecular-beam epitaxy (MBE) [7]. Among these methods, MBE can be used to grow samples in high vacuum, which is important when preparing crystalline materials. Indeed, device quality ZnSe epitaxial layers reported in the literature were all prepared by MBE [8–10]. With the ability to precisely control growth parameters and to accurately monitor growth process, MBE should be an ideal tool to grow nano-structured materials.

For conventional 2D devices, heterostructure plays a very important role. Similarly, the concept of heterostructure can be applied to 1D nanowires/tips. Indeed, GaN/InGaN, InAs/InP, Si/SiGe, and ZnMgO/ZnO heterostructure nanowires/tips have all been demonstrated [11–14]. It is also possible to prepared nanowires/tips with superlattice structure. For these superlattice nanowires/tips, the longitudinal confinement could couple with radial confinement. This should provide more functionalities for the superlattice nanowires/tips [15]. To realize ZnSe-based superlattice nanowires/tips, it is necessary to form ternary nanowires/

tips. Very recently, we reported the growth of ternary ZnSeTe nanotips by MBE and the fabrication of a ZnSeTe nanotip-based photodetector [16]. ZnSeTe is a ternary material with interesting optical properties. It has been shown that strong luminescence signal could be observed from localized excitons bound to Te atom ($Te_1$ emission) and $Te_n$ ($n \geq 2$) cluster ($Te_n$ cluster emission) in 2D ZnSeTe epilayer [17, 18]. In this study, we report the growth of ZnSe/ZnSeTe superlattice nanotips by MBE on oxidized Si(100) substrates. Physical and optical properties of the ZnSe/ZnSeTe superlattice nanotips will be discussed.

## Experimental

The ZnSe/ZnSeTe superlattice nanotips used in this study were grown by a Riber 32P solid source MBE system on oxidized Si(100) substrate using vapor–liquid–solid (VLS) mechanism with an Au-based nano-catalyst. The source materials for the MBE system were elemental Zn (6N), Se (6N) and Te (6N). Prior to the growth of the nanotips, a Si(100) substrate was first immersed in boiled acetone for 10 min, in boiled isopropyl alcohol for 10 min, and in hydrofluoric acid solution for 30 s. The chemically cleaned Si substrate was thermally oxidized to form a 150-nm-thick $SiO_2$ film. This $SiO_2$ film acts as a catalyst diffusion barrier [19]. A 0.6-nm-thick Au film was then deposited onto the $SiO_2$ layer by sputtering. The sample was then loaded onto the preparation chamber and annealed at 280°C to transfer Au film into Au nano-particles [20]. Subsequently, the substrate was transferred into the growth chamber to grow the ZnSe/ZnSeTe superlattice nanotips at 280°C for 1 h.

It has been shown previously that ZnSe nanowires can be grown by MBE based on Au-catalyzed VLS deposition [7]. Similar growth mechanism should be applied to the growth of ZnSe/ZnSeTe superlattice nanotips in this study. Figure 1a shows schematic diagram of the VLS growth of ZnSe/ZnSeTe superlattice nanotips. With Au nano-particles dispersed on the oxidized Si substrate, eutectic Au–Zn alloy droplets were first formed. The deposited source atoms (i.e., Zn, Se, and Te) were then diffused along the nanotip sidewalls to form the ZnSe/ZnSeTe superlattice nanotips. During the growth, we carefully controlled the growth time so as to achieve the designated thickness. We also carefully controlled beam equivalent pressures of Zn, Se, and Te so as to keep the composition ratio at Se:Te = 9:1. We prepared samples with three different ZnSeTe well layer thickness (i.e., $Lw = 16$, 20, and 24 nm) while the ZnSe barrier layer thickness was kept at 78 nm. The schematic diagram of the ZnSe/ZnSeTe superlattice nanotips grown on oxidized Si (100) substrate is shown in Fig. 1b. Growth interruptions were also

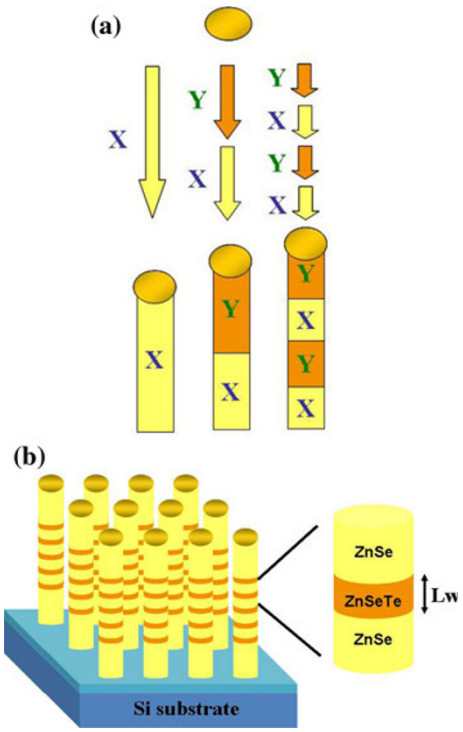


**Fig. 1** Schematic diagrams of **a** the VLS growth of ZnSe/ZnSeTe superlattice nanotips and **b** the ZnSe/ZnSeTe superlattice nanotips grown on oxidized Si (100) substrate

introduced at each ZnSe/ZnSeTe interface by stopping the growth for 30 s.

After the growth, surface morphologies of the samples were characterized by a Hitachi S-4700I field-emission scanning electron microscope (FESEM) operated at 15 kV. A Philips FEI TECNAI $G^2$ high resolution transmission electron microscopy (HRTEM) operated at 200 kV and a Siemens D5000 X-ray Diffraction (XRD) system were applied to analyze crystallographic and structural properties of these superlattice nanotips. To characterize optical properties, photoluminescence (PL) measurements were performed by a continuous wave (CW) He–Cd laser operated at 325 nm as the excitation source. The luminescence signals generated from the samples were then recorded by a lock-in amplifier at 20 to 100 K.

## Results and Discussion

Figure 2a–c show top-view FESEM images of the ZnSe/ZnSeTe superlattice nanotips with $Lw = 16$, 20, and 24 nm, respectively. As shown in these figures, it was found that high density nanotips were successfully grown on the oxidized Si(100) substrate. Insets in these figures show the respective enlarged FESEM images. As shown in these insets, it was found that average length of these nanotips was 0.95 μm.

Figure 3 show HRTEM image of one randomly selected ZnSe/ZnSeTe superlattice nanotip with $Lw = 20$ nm. Fast Fourier transform (FFT) patterns measured from four different points in this particular superlattice nanotip were shown at the bottom of this figure [21, 22]. Among the four points, points 2 and 3 were from the $ZnSe_{0.9}Te_{0.1}$ well layer while points 1 and 4 from the ZnSe barrier. It can be seen from FFT patterns measured from points 1 and 4, it was found that the crystal was grown along the [111] lattice direction in these two points. This indicates that points 1 and 4 (i.e., ZnSe barrier layers) exhibit cubic zinc-blende structure. In contrast, the crystal was grown along the [220] lattice direction in points 2 and 3. This indicates that points 2 and 3 (i.e., ZnSeTe well layers) exhibit hexagonal wurtzite structure. In other words, we can change the crystal structure from zinc-blend to wurtzite by introducing 10% Te into the nanowires. From the HRTEM image, it can be seen that the interfaces between zinc-blende and wurtzite domains were sharp with very few defects. The sharp interfaces observed in this HRTEM image should be attributed to the use of growth interruption at each ZnSe/ZnSeTe interface. Inset in Fig. 3 shows low-magnification bright-field TEM image of one single nanotip. It was found that an eutectic Au nanoparticle existed on the tip, which confirms that these nanotips were indeed formed by the VLS mechanism.

Figure 4 shows XRD spectra measured from the three ZnSe/ZnSeTe superlattice nanotips. It was found that the XRD peaks observed in these three samples could all be indexed to the cubic zinc-blende (111), (220), (311) peaks and the hexagonal wurtzite (103) and (002). These peaks again indicate that our ZnSe/ZnSeTe superlattice nanotips exhibit mixture of zinc-blende and wurtzite structures. It

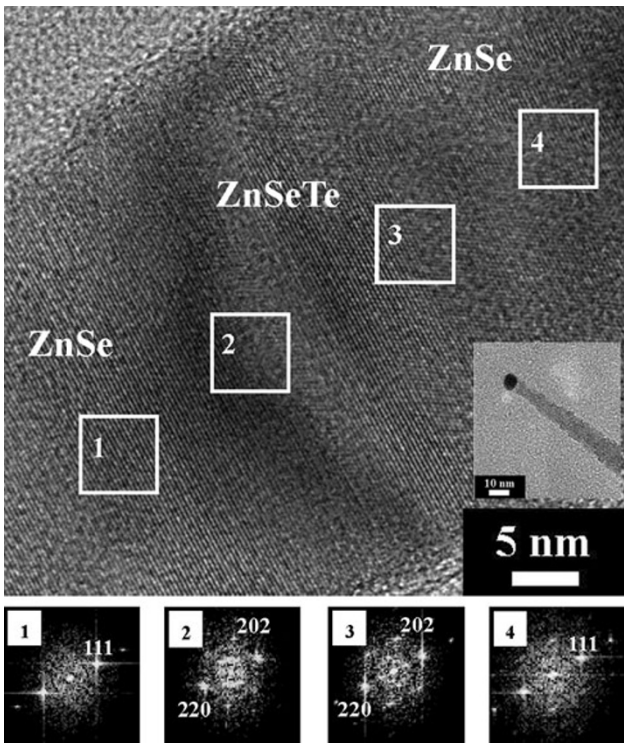


**Fig. 3** HRTEM image of one randomly selected ZnSe/ZnSeTe superlattice nanotip with $Lw = 20$ nm. Insets at the bottom show FFT patterns measured from four different points in this particular superlattice nanotip and low-magnification bright-field TEM image

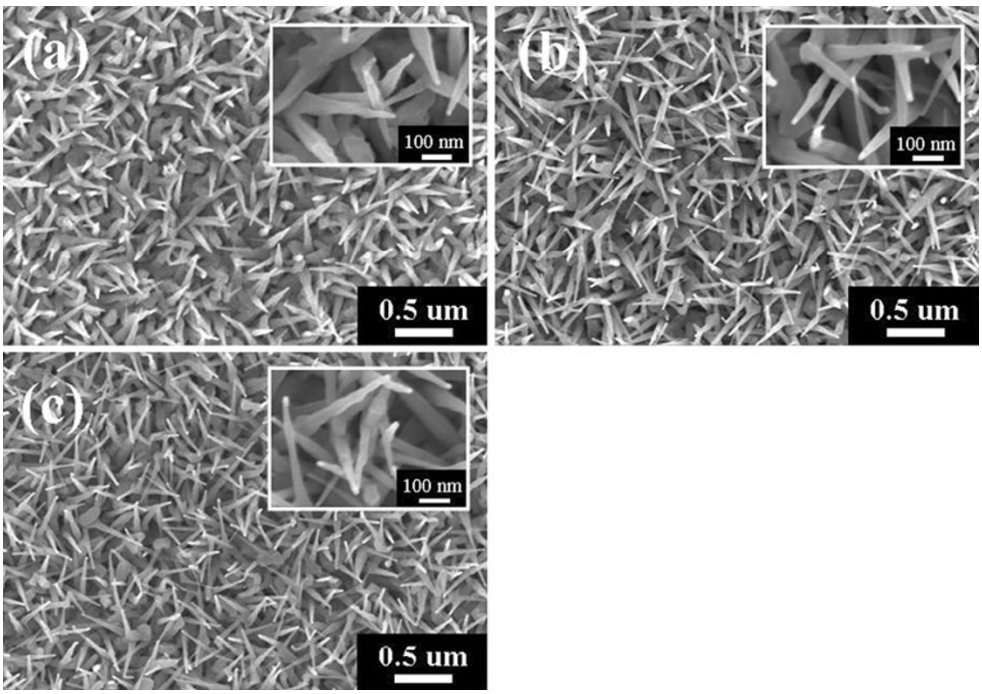


**Fig. 2** Top-view FESEM images of the ZnSe/ZnSeTe superlattice nanotips with $Lw =$ **a** 16 nm, **b** 20 nm, and **c** 24 nm, respectively

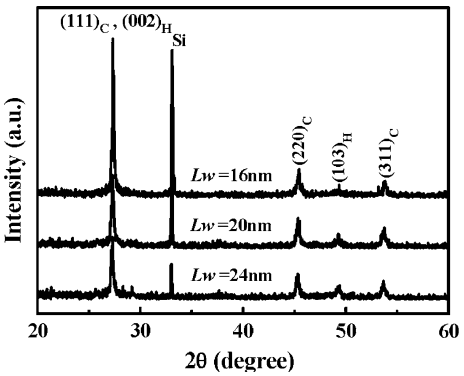


**Fig. 4** XRD spectra measured from the three ZnSe/ZnSeTe superlattice nanotips

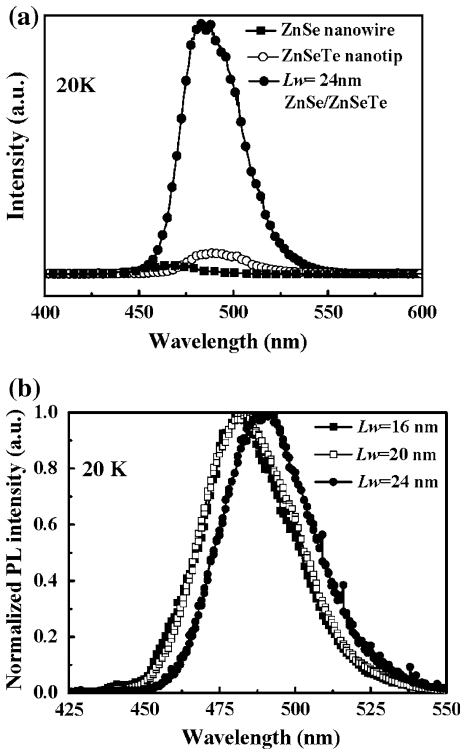


**Fig. 5** **a** PL spectrum of the ZnSe/ZnSeTe superlattice nanotips measured at 20 K. PL spectra of ZnSe nanowires and ZnSeTe nanotip were also plotted for comparison. **b** Normalized PL spectra of the three ZnSe/ZnSeTe superlattice nanotips measured at 20 K

can also be seen that full-width-half-maxima (FWHMs) of the observed XRD (111) peaks were 0.2°, 0.26° and 0.32° for the samples with $Lw = 16$, 20 and 24 nm, respectively. The small FWHMs suggest reasonably good crystal quality of our ZnSe/ZnSeTe superlattice nanotips.

Figure 5a shows PL spectrum of the ZnSe/ZnSeTe nanotips measured at 20 K. It was found that the 20 K PL peak of the ZnSe/ZnSeTe nanotips prepared in this study was located at 491 nm (i.e., 2.53 eV) with a 31 nm FWHM. For comparison, PL spectra of ZnSe nanowires and ZnSeTe nanotips were also plotted in the same figure. It was found that PL peak positions were located at 467 nm (i.e., 2.66 eV) and 492 nm (i.e., 2.52 eV) while PL peak FWHMs were 29 and 30 nm for the ZnSe nanowires and the ZnSeTe nanotips, respectively [16, 17]. Figure 5b shows normalized PL spectra of the three ZnSe/ZnSeTe nanotips measured at 20 K. It was found that PL peaks occurred at 482, 484, and 491 nm for the ZnSe/ZnSeTe nanotips with $Lw = 16$, 20, and 24 nm, respectively. In other words, the PL peak blue-shifted by 9 nm as we decreased the ZnSeTe well layer thickness, $Lw$, from 24 to 16 nm. This should be attributed to the quantum confinement effect [23]. It should be noted that PL intensities observed from these ZnSe/ZnSeTe superlattice nanotips were all much larger than that observed from the homogeneous ZnSeTe nanotips prepared with the same method and with the same Te composition ratio [16]. The much larger PL intensities should be attributed to the effective confinement of carriers in the well layers.

Figure 6a–c shows Arrhenius plots of the integrated PL intensities measured from the ZnSe/ZnSeTe superlattice nanotips with $Lw = 16$, 20, and 24 nm, respectively. It was found that we can fit the experimental data since the temperature dependence of the integrated PL intensities could be expressed as follows [24]:

$$I(T) = \frac{I_0}{1 + A\exp(-E_A/kT)} \quad (1)$$

where $I_0$ is the integrated PL intensity at low temperatures, $k$ is the Boltzmann's constant, $T$ is temperature, $A$ is rate constants while $E_A$ is the activation energy, respectively. As shown in Fig. 6a–c, it was found that activation energies were 76, 46, and 19 meV for the ZnSe/ZnSeTe superlattice nanotips with $Lw = 16$, 20, and 24 nm, respectively. It should also be noted that these values were all larger than that observed from the previously reported homogeneous ZnSe nanowires [16]. At high temperatures, PL quenching in quantum wells is primarily due to the thermal emission of charge carriers from the confined quantum well states into the barrier states [25]. Compared with homogeneous ZnSe nanowires, the larger activation energies observed in Fig. 6a–c suggest that the ZnSe/ZnSeTe superlattice nanowires reported in this study are potentially useful for feasible nano-photonic application. To overcome the quenching effect, we need to improve crystal quality of these nanotips. One possible method is to grow these nanotips on lattice matched ZnSe/GaAs template instead of oxidized Si substrate. Such an experiment is underway and the results will be reported separately.

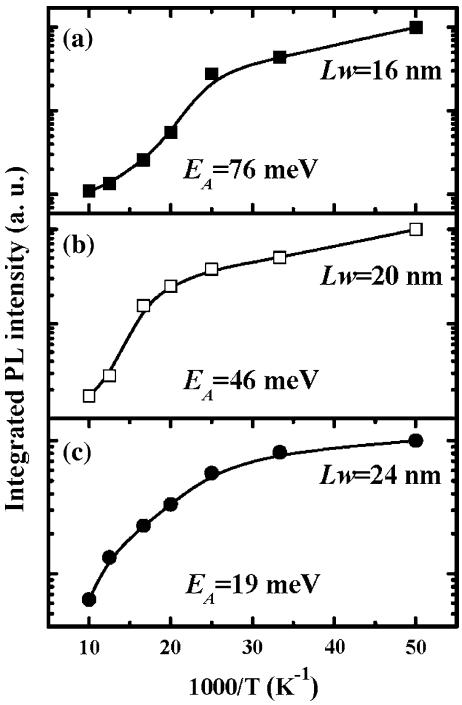


**Fig. 6** Arrhenius plots of the integrated PL intensities measured from the ZnSe/ZnSeTe superlattice nanotips with $Lw$ = **a** 16 nm, **b** 20 nm, and **c** 24 nm

## Conclusions

In summary, we reported the growth of ZnSe/ZnSeTe superlattice nanotips on oxidized Si(100) substrate by MBE using VLS mechanism with an Au-based nanocatalyst. It was found that the ZnSe/ZnSeTe superlattice nanotips exhibit mixture of cubic zinc-blende and hexagonal wurtzite structures. It was also found that PL intensities observed from the ZnSe/ZnSeTe superlattice nanotips were significantly larger than that observed from the homogeneous ZnSeTe nanotips.

**Acknowledgments** This study was supported in part by the Center for Frontier Materials and Micro/Nano Science and Technology and in part by the Advanced Optoelectronic Technology Center, National Cheng Kung University, under projects from the Ministry of Education. This study was also in part supported by Ministry of Economic Affairs (MOEA) and NSC 98-EC-17-A-09020769. The authors would like to thank the Bureau of Energy, Ministry of Economic Affairs of R.O.C. for financially supporting this research under Contract No. 98-D0204-6 and the LED Lighting and Research Center, NCKU for the assistance regarding measurements.



## References

1. W.R. Chen, S.J. Chang, Y.K. Su, J.F. Chen, W.H. Lan, W.J. Lin, Y.T. Cherng, C.H. Liu, U.H. Liaw, IEEE Photon. Technol. Lett. **14**, 1061 (2002)
2. S. Taniguchi, T. Hino, S. Itoh, K. Nakano, N. Nakayama, A. Ishibashi, M. Ikeda, Electron. Lett. **32**, 552 (1996)
3. S.J. Chang, Y.K. Su, W.R. Chen, J.F. Chen, W.H. Lan, W.J. Lin, Y.T. Cherng, C.H. Liu, U.H. Liaw, IEEE Photon. Technol. Lett. **14**, 188 (2002)
4. T.W. Zhang, Y.Q. Shen, W. Hu, J. Sun, J. Wu, Z.F. Ying, N. Xu, J. Vacuum Sci. Technol. **25**, 1823 (2007)
5. X.T. Zhang, Z. Liu, Y.P. Leung, Q. Li, S.K. Hark, Appl. Phys. Lett. **83**, 5533 (2003)
6. B. Xiang, H.Z. Zhang, G.H. Li, F.H. Yang, F.H. Su, R.M. Wang, J. Xu, G.W. Lu, X.C. Sun, Q. Zhao, D.P. Yu, Appl. Phys. Lett. **82**, 3330 (2003)
7. A. Colli, S. Hofmann, C. Ferrari, F. Ducati, F. Martelli, S. Rubini, S. Cabrini, A. Franciosi, J. Robertson, Appl. Phys. Lett. **86**, 153103 (2005)
8. H. Ishikura, N. Fukuda, M. Itoi, K. Yasumoto, T. Abe, H. Kasada, K. Ando, J. Crystal Growth **214**, 1130 (2000)
9. C.S. Yang, M.C. Kuo, Y.J. Lai, K.C. Chiu, J.L. Shen, J. Lee, W.C. Chou, S.Y. Jeng, W.H. Lan, Mater. Chem. Phys. **81**, 1 (2003)
10. C.D. Lee, H.L. Park, C.H. Chung, S.K. Chang, Phys. Rev. B **45**, 4491 (1992)
11. H.M. Kim, T.W. Kang, K.S. Chung, Adv. Mater. **15**, 567 (2003)
12. M.T. Bjork, B.J. Ohlsson, T. Sass, A.I. Persson, C. Thelander, M.H. Magnusson, K. Deppert, L.R. Wallenberg, L. Samuelson, Nano. Lett. **2**, 87 (2002)
13. Y.Y. Wu, R. Fan, P.D. Yang, Nano Lett **2**, 83 (2002)
14. W.I. Park, G.C. Yi, M. Kim, S.J. Pennycook, Adv. Mater. **15**, 526 (2003)
15. J. Yan, X. Fang, L. Zhang, Y. Bando, U.K. Gautam, B. Dierre, T. Sekiguchi, D. Golberg, Nano Lett **8**, 2794 (2008)
16. S.J. Chang, C.H. Hsiao, S.C. Hung, S.H. Chih, B.W. Lan, S.B. Wang, S.P. Chang, Y.C. Cheng, T.C. Li, B.R. Huang, J. Electrochem. Soc. **157**, K1 (2010)
17. C.S. Yang, D.Y. Hong, C.Y. Lin, W.C. Chou, C.S. Ro, W.Y. Uen, W.H. Lan, S.L. Tu, J. Appl. Phys. **83**, 2555 (1998)
18. M. Kishino, S. Tanaka, K. Senda, Y. Yamada, T. Taguchi, J. Crystal Growth **214/215**, 220 (2000)
19. S. Hofmann, C. Ducati, R.J. Neill, S. Piscanec, A.C. Ferrari, J. Geng, R.E. Dunin-Borkowski, J. Robertson, J. Appl. Phys. **94**, 6005 (2003)
20. M. Tchernycheva, G.E. Cirlin, G. Patriarche, L. Travers, V. Zwiller, U. Perinetti, J.C. Harmand, Nano. Lett. **7**, 1500 (2007)
21. D.L. Dheeraj, G. Patriarche, L. Largeau, H.L. Zhou, A.T.J. van Helvoort, F. Glas, J.C. Harmand, B.O. Fimland, H. Weman, Nanotechnol **19**, 1275605 (2008)
22. D.B. Mitzi, Inorg. Chem. **44**, 7078 (2005)
23. W.I. Park, S.J. An, J.L. Yang, G.C. Yi, S. Hong, T. Joo, M. Kim, J. Phys. Chem. B **108**, 15457 (2004)
24. A. Yasan, R. McClintock, K. Mayes, D.H. Kim, P. Kung, M. Razeghi, Appl. Phys. Lett. **83**, 4083 (2003)
25. E. Tournie, C. Morhain, M. Leroux, C. Ongaretto, J.P. Faurie, Appl. Phys. Lett. **67**, 103 (1995)